Biosensors and Bioelectronics 26 (2010) 1346–1352

Contents lists available at ScienceDirect

Biosensors and Bioelectronics

journal homepage: www.elsevier.com/locate/bios

Nanoparticle-based biosensor for the detection of emerging pandemic influenza strains

Tracy L. Kamikawa[a,b], Malgorzata G. Mikolajczyk[b], Michael Kennedy[b], Pei Zhang[b], Wei Wang[c], Dorothy E. Scott[b], Evangelyn C. Alocilja[a,*]

[a] Department of Biosystems and Agricultural Engineering, Michigan State University, East Lansing, MI 48824, USA
[b] United States Food and Drug Administration, Center for Biologics Evaluation and Research, Bethesda, MD 20892, USA
[c] Department of Crop and Soil Sciences, Michigan State University, East Lansing, MI 48824, USA

ARTICLE INFO

Article history:
Received 14 April 2010
Received in revised form 7 July 2010
Accepted 13 July 2010
Available online 21 July 2010

Keywords:
Influenza
Biosensor
Direct-charge transfer
Electrically active
Immunomagnetic
Polyaniline

ABSTRACT

Electrically active magnetic (EAM) nanoparticles, consisting of aniline monomer polymerized around gamma iron(III) oxide (γ-Fe_2O_3) cores, serve as the basis of a direct-charge transfer biosensor developed for detection of surface glycoprotein hemagglutinin (HA) from the Influenza A virus (FLUAV) H5N1 (A/Vietnam/1203/04). H5N1 preferentially binds α2,3-linked host glycan receptors. EAM nanoparticles were immunofunctionalized with antibodies against target HA. Glycans preincubated with HA in 10% mouse serum were incubated with anti-HA–EAM complexes. The anti-HA–EAM complexes effectively acted as immunomagnetic separator of HA from mouse serum matrix. EAM nanoparticles served as the biosensor transducer for cyclic voltammetry measurements. The polyaniline was made electrically active by hydrochloric acid doping. Experimental results indicate that the biosensor is able to detect recombinant H5 HA at 1.4 μM in 10% mouse serum, with high specificity for H5 as compared to H1 (H1N1 A/South Carolina/1/18). This novel design applies EAM nanoparticles in a sensitive, specific, affordable, and easy-to-use biosensor with applications in disease monitoring and biosecurity.

1. Introduction

The recent swine-origin H1N1 pandemic has brought attention to Influenza A virus (FLUAV), a causative agent of influenza infection. FLUAV of various virulence and strains has long been the cause of worldwide pandemics and common annual epidemics of respiratory tract infections (Werner and Harder, 2006). Globally, FLUAV annually affects millions of people and also impacts various animal species. The surface glycoproteins hemagglutinin (HA) and neuraminidase (NA) characterize each strain by serotype. HA dictates host specificity and host cell entry, determining the extent of host infection. Of the sixteen known HA and nine NA serotypes, all circulate in the avian population, leading to the common belief that birds act as the main FLUAV reservoir (Stevens et al., 2006; Webster et al., 1992; Wiley and Skehel, 1987). Highly pathogenic H5N1 has presented a continuous threat throughout Asia, Europe, and Africa since 2003, with sporadic related infections in humans (Magalhaes et al., 2010). Three HA and two NA have adapted sufficiently to become human-transmissible, namely H1N1, H2N2, H3N2, and H1N2 (Neumann et al., 2010).

Antigenic drift causes seasonal influenza epidemics, resulting in 36,000 deaths and costs of $10 billion in the U.S. annually (HSC, 2005). Antigenic pressure from the prominent circulating HA type generates minor changes in HA (Wright and Webster, 2001). Antigenic shifts cause global, high-mortality FLUAV pandemics when the genomic RNA segment encoding HA is replaced, allowing rapid inter-species adaptation (Gurtler, 2006). Of the historical pandemic strains, the 1918–1919 H1N1 "Spanish flu" was the most virulent, causing 20–40 million deaths (Reid et al., 2001; Stevens et al., 2006). The 2009 H1N1 pandemic originated from a swine FLUAV that has been circulating in pig herds for decades, demonstrating how quickly a human-transmissible FLUAV can spread (Michaelis et al., 2009).

Transmission of FLUAV infections, and thus pandemic potential, is dependent upon HA receptor specificity for host glycan receptors. Avian FLUAV preferentially bind sialic acid-terminated glycans with α2,3-linkages to galactose, whereas human FLUAV preferentially bind to α2,6-linkages. Avian FLUAV are of concern to human health due to the widely held belief that a highly pathogenic avian FLUAV could achieve human infectivity, transmissibility, and pandemic potential due to antigenic shifting (Blixt et al., 2004; Stevens et al., 2006).

* Corresponding author at: Department of Biosystems and Agricultural Engineering, Michigan State University, 115 Farrall Hall, East Lansing, MI 48824, USA.
Tel.: +1 517 432 8672; fax: +1 517 432 2892.
E-mail address: alocilja@msu.edu (E.C. Alocilja).

0956-5663/$ – see front matter © 2010 Elsevier B.V. All rights reserved.
doi:10.1016/j.bios.2010.07.047

Influenza virus is typically analyzed by well established conventional virological methods (Amano and Cheng, 2005). Viral isolation culture with immunocytological confirmation remains the "gold standard." Other methods include hemagglutination-inhibition (HI), which is gaining preference for WHO global surveillance; microneutralization; complement fixation; RT-PCR; and ELISA (Table A1). These methods offer high sensitivity and specificity, yet require hours to days for culture and detection.

Influenza antigens or enzymes may also be directly detected by commercial diagnostic test kits. Few differentiate between influenza A and B. These kits require 30 min for testing with sensitivity from 51 to 87% and specificity from 69 to 99% (Table A2) (Amano and Cheng, 2005; Faix et al., 2009). These methods reveal a need for rapid technology which offers quantitative results as opposed to subjective color change assessments.

A biosensor quantifies a physiological or biochemical change in terms of an electrical response by integrating a biological component with an electronic, electrochemical, optical, or acoustic transducer (D'Souza, 2001; Muhammad-Tahir et al., 2007; Pal et al., 2007, 2008a,b; Pal and Alocilja, 2009; Turner et al., 1987). Various biosensors have been described in the literature, but there remains a need for a biosensor technology with rapid, quantitative, robust, in-field capabilities for point-of-care FLUAV detection.

Polyaniline is a highly studied conducting polymer in a family that includes polypyrrole, polyacetylene, and polythiophene. As both electrical conductor and organic compound, polyaniline possesses flexibility, robustness, highly controllable properties, simple synthesis, low cost, and environmental stability. Addition of a protic solvent such as hydrochloric acid yields a conducting form of polyaniline, with a conductivity increase of up to ten orders of magnitude (Ahuja et al., 2007; Sarno et al., 2005). Polyaniline offers efficient electronic charge transfer, making it attractive for biosensor application (Catolla et al., 2006; Kuwabata et al., 2005; Scott et al., 2005). Magnetic polyaniline nanoclusters have been prepared with magnetic core materials of iron(II, III) oxide, hydroxyl iron, and Li Ni ferrite (Baker et al., 2004; Dallas et al., 2006; Poddar et al., 2004; Xue et al., 2006; Zhang et al., 2005).

The main objective of this study is the novel application of electrically active magnetic (EAM) polyaniline nanostructures as magnetic concentrator and signal transducer in a biosensor for rapid detection of emerging pandemic FLUAV strains. To our knowledge, this is the first time such a biosensor architecture is reported. Our biosensor design utilizes EAM nanoparticles as the electrical transducer and monoclonal antibodies as the biological sensing element on single-use, portable, highly sensitive screen-printed carbon electrodes (SPCEs), which consist of carbon working and silver/silver chloride reference electrodes printed on low-cost polymer backing (Fig. 1a) (Dominguez Renedo et al., 2007; Susmel et al., 2003). Here we present a novel method of magnetic separation and direct electrical detection in the development of an electrochemical biosensor for rapid, sensitive, and specific detection of FLUAV HA. We investigate proof-of-concept binding between purified recombinant HA and synthetic carbohydrate receptor mimics.

2. Materials and methods

2.1. Glycans, HA, and antibodies

Biotinylated carbohydrate compounds 3′SLe^x (B157), 3′SLN (B84), GT3 (B108), and 6′SLN (B87) were provided by the Carbohydrate Synthesis/Protein Expression Core of The Consortium for Functional Glycomics funded by the National Institute of General Medical Sciences grant GM62116. The following reagents were obtained through the NIH Biodefense and Emerging Infections Research Resources Repository, NIAID, NIH: (1) H5 hemagglutinin (HA) protein from Influenza Virus, A/Vietnam/1203/04 (H5N1), recombinant from baculovirus, NR-10510 (Source A H5, referred to as H5) and (2) monoclonal anti-influenza virus H5 hemagglutinin (HA) protein (VN04-2), A/Vietnam/1203/04 (H5N1) (ascites, Mouse), NR-2728. The following were purchased from Immune Technology Corp. (New York, NY): (1) 6xHis tagged H5 hemagglutinin (HA) protein from 293 cell culture, A/Vietnam/1203/04 (H5N1) (Source B H5, referred to as H5*); (2) C-terminal 6xHis tagged H1 hemagglutinin (HA) protein from 293 cell culture, A/South Carolina/1/18 (H1N1); and (3) polyclonal anti-influenza virus H1 hemagglutinin (HA) protein, H1N1/Pan (rabbit).

2.2. Chemicals and reagents

Solutions and buffers used in the biosensor study were prepared in deionized (DI) water (Millipore Direct-Q system). Iron(III) oxide (γ-Fe_2O_3) nanopowder, aniline monomer, ammonium persulfate, hydrochloric acid (HCl), methanol, diethyl ether, hydrogen tetrachloroaurate(III) trihydrate, sodium citrate dehydrate, glutaraldehyde, Polysorbate-20 (Tween-20), phosphate buffered saline (PBS), trizma base, casein, sodium phosphate (dibasic and monobasic), and streptavidin were purchased from Sigma–Aldrich (St. Louis, MO). Solutions were prepared as follows: PBS buffer (10 mM PBS, pH 7.4), wash buffer (10 mM PBS, pH 7.4, with 0.05% Tween-20), phosphate buffer (100 mM phosphate buffer, pH 7.4), casein blocking buffer (100 mM Tris–HCl buffer, pH 7.6, with 0.1%, w/v casein), and glycine blocking buffer (67 μM glycine in 10 mM PBS, pH 7.4). HBS–P buffer, 10 mM glycine pH 2.5, and 50 mM NaOH were purchased from GE Healthcare (Piscataway, NJ). Avidin/biotin blocking kit was purchased from Vector Laboratories, Inc. (Burlingame, CA).

2.3. Gold nanoparticle synthesis

Application of carbon-based glycans directly onto the SPCE would be insulating. To enhance the electron transducer, thus amplifying response current, gold nanoparticles (AuNPs) were applied to the SPCEs (Daniel and Astruc, 2004; Lin et al., 2008; Willner et al., 2007). AuNPs were synthesized according to published procedure and have been previously characterized (Hill and Mirkin, 2006; Zhang et al., 2009). Hydrogen tetrochloroaurate(III) trihydrate aqueous solution (1 mM, 50 ml) was stirred while heated to vigorous reflux, followed by titration with 5 ml of 38.8 mM sodium citrate. The solution shifted from yellow to deep red.

2.4. EAM polyaniline nanostructure synthesis

Aniline monomer was polymerized around gamma iron(III) oxide (γ-Fe_2O_3) cores to obtain magnetic/polyaniline core/shell (c/s) nanoparticles (Sharma et al., 2005). Commercially manufactured γ-Fe_2O_3 nanoparticles were sonicated and dispersed in 50 ml of 1 M HCl, 10 ml deionized (DI) water, and 0.4 ml aniline monomer at 0 °C for 1 h. The γ-Fe_2O_3: monomer weight ratio was fixed at 1:0.6. 1 g ammonium persulfate in 20 ml DI water was added as oxidant while the mixture was stirred at 0 °C. As electrically active polyaniline, typically green, was formed over the γ-Fe_2O_3 nanoparticles, typically brown, the solution visibly transitioned from rust brown to dark green. The reaction proceeded for 4 h with continuous stirring at 0 °C. The solution was filtered, washed with 1 M HCl, 10% methanol, and diethyl ether, and dried for 18 h. The resulting green solid was ground into fine powder and stored in a vacuum desiccator. The NPs have been previously characterized in terms of structure, size, magnetization, and conductivity (Pal et al., 2008a; Pal and Alocilja, 2009).

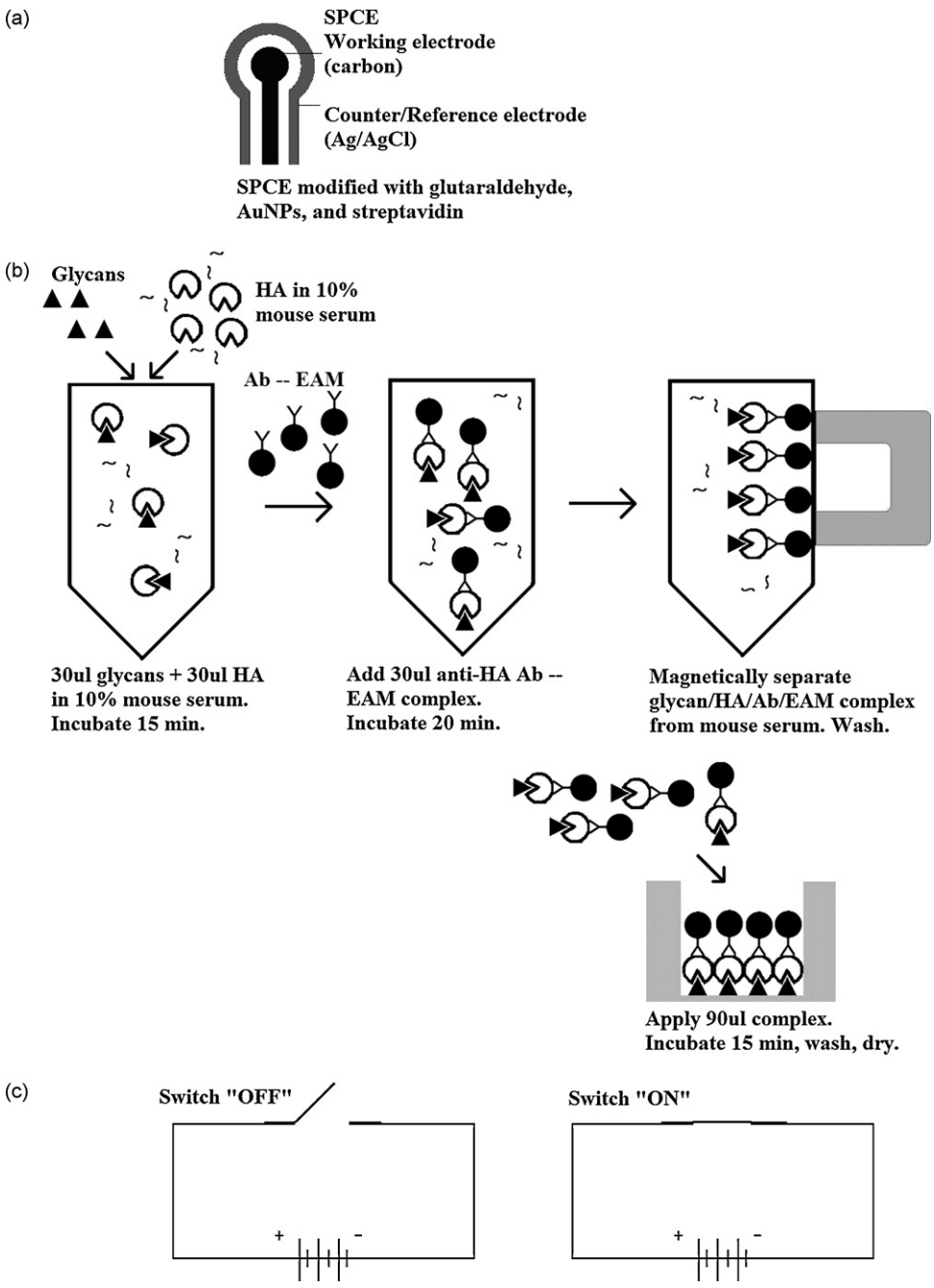

Fig. 1. SPCE testing schematic. (a) Screen-printed carbon electrode (SPCE): carbon working and silver/silver chloride counter/reference electrodes, (b) preconcentration preparation, and (c) schematic of the corresponding electrical circuit before and after analyte application.

2.5. EAM immunofunctionalization

EAM nanoparticles were immunofunctionalized with α-H5 monoclonal antibody IgG2 or α-H1 polyclonal antibody. Desiccated EAM polyaniline nanoparticles were dissolved in 100 mM phosphate buffer (pH 7.4) to 10 mg/ml, and sonicated for 15 min. The EAM polyaniline nanoparticles were conjugated with α-H5 monoclonal antibodies by direct physical adsorption (Pal and Alocilja, 2009). α-H5 monoclonal antibody or α-H1 polyclonal antibody was added to the EAM polyaniline nanoparticles to obtain an antibody: EAM ratio of 1:10 (v/v). The solution was incubated for 1 h at 25 °C in a rotational hybridization oven (Amerex Instruments, Inc., Lafayette, CA). The immunofunctionalized nanoparticles were magnetically separated using a FlexiMag Magnetic Separator (Spherotech, Inc., Lake Forest, IL) to remove any unbound antibody, and washed twice with blocking buffer of 100 mM Tris–HCl buffer (pH 7.6) with 0.1% (w/v) casein with magnetically separated supernatant discarded. The anti-HA–EAM complexes were resuspended in 100 mM phosphate buffer (pH 7.4) on the day of testing.

2.6. SPCE modification

SPCE chips were prepared by removing the overlaying mesh and foam (Gwent, Inc., UK). Each chip was washed with 2 ml sterile DI water and air dried at 25 °C for 15 min. The working area was treated with 25 μl of 2.5 mM glutaraldehyde solution and 25 μl of AuNP solution at 4 °C for 1 h each, with wash and air dry after each

Table 1
Saccharide sequences and predicted binding to H5N1.

Saccharide name, synthetic spacer	Common name	Predicted to bind H5N1
Neu5Acα2-3Galβ1-4[Fucα1-3]GlcNAcβ-SpNH-LC-LC-Biotin	3′Slex	Yes
Neu5Acα2-3Galβ1-4GlcNAcβ-SpNH-LC-LC-Biotin	3′SLN	Yes
Neu5Acα2-8Neu5Acα2-8Neu5Acα2-3Galβ1-4Glcβ-SpNH-LC-LC-Biotin	GT3	No
Neu5Acα2-6Galβ1-4GlcNAcβ-SpNH-LC-LC-Biotin	6′SLN	No

(Lin et al., 2008). 20 μl of streptavidin at 1 μg/ml were applied to the working area and dried at 4 °C for 2 h.

2.7. Sample preparation: preconcentration

Glycans and HAs were prepared at 3 times the desired concentration in 0.01 M PBS. HAs contained 10% mouse serum (ICR SCID) (v/v). 30 μl of each were incubated for 15 min at 25 °C in a rotational hybridization oven. 30 μl of the appropriate anti-HA–EAM complex was then added to the glycan/HA solution and rotationally incubated for 20 min at 25 °C. The glycan/HA/anti-HA–EAM complexes were magnetically separated and washed twice with 0.01 M PBS containing 0.05% Tween-20 for 5 min and resuspended in 0.01 M PBS.

2.8. Capture experiments: preconcentration

The SPCE chips prepared with glutaraldehyde, AuNPs, and streptavidin were then treated with the biotinylated glycan/HA/anti-HA–EAM complex. 90 μl of the solution was applied to the treated SPCE and incubated at 25 °C for 15 min. The SPCE was washed with 2 ml DI water and air dried at 25 °C for 15 min (Fig. 1b).

2.9. Biosensor testing apparatus

Cyclic voltammetric measurements were performed by a 263A potentiostat/galvanostat (Princeton Applied Research, MA, USA). Data collection and analysis were controlled through the PowerSuite electrochemical software operating system (Princeton Applied Research, Wellesley, MA).

2.10. Detection and data analysis

100 μl of 0.1 M HCl solution were applied over the SPCE electrode area and incubated for 5 min. Each SPCE electrode was connected to the potentiostat and cyclic voltammetry was performed at 55 mV/s scan rate over −0.4 to 1 V scan range, with four consecutive 2 min scans recorded. Previous experimentation indicated that the third scan produced the most pronounced difference in current flow for different samples and was chosen for analysis. Each sample was performed in three replications. The samples were calibrated against a negative control of the anti-HA–EAM application step alone. The total charge transferred, ΔQ, was computed from the cyclic voltammogram as the integral of current, according to the relationship:

$$I = \frac{\Delta Q}{\Delta t} \quad (1)$$

where I is the current (A), ΔQ is the charge transferred (C), and Δt is the time elapsed (s) (Kuznetsov, 1995). Standard deviations and mean ΔQ values of the third scans for the triplicate data sets were calculated.

Presence of target is indicated by an increase in total charge transferred between the redox of polyaniline and the working electrode. Target HA labeled with the immunofunctionalized EAMs were captured on the SPCE surface, and the EAMs, consisting of conductive polyaniline synthesized around a magnetic γ-Fe_2O_3 core, formed an electrical circuit between the silver electrodes, with current recorded by the potentiostat (Fig. 1c).

2.11. Biosensor sensitivity and specificity testing

The lowest detection limit of the biosensor for H5 was investigated using three samples at 1:2 dilution in 0.01 M PBS to obtain H5 at 1.4 μM, 700 nM, and 360 nM. Anti-HA–EAM complexes alone were tested as controls. The lowest dilution of H5 that produced a signal distinguishable from the control was taken as the sensitivity of detection.

The specificity of the biosensor was investigated using H1, α-H1, and glycans nonspecific for H5, GT3 (α2,8 binder) and 6′SLN (α2,6 binder). The H1 was prepared at 1.4 μM in 0.01 M PBS, the non-H5 binding glycans were prepared at 100 μM, and the EAMs were immunofunctionalized with α-H1 at 1:10 using the method described in Section 2.6.

Biological sample complexity for ultimate application in in-field blood or sputum testing was considered in the preconcentration method. HA samples were prepared with 10% mouse serum. After complexing the glycan/HA/anti-HA–EAM, the magnetic separation and washing technique was utilized to specifically isolate target HA from complex serum matrix.

2.12. Statistical analysis

Each sample was tested in triplicate with the disposable biosensors to nullify equipment or user variation effects. The prepared biosensors were assumed to have the same physical properties. The mean and standard deviations of the ΔQ values were calculated. The differences between the means were calculated and analyzed based on single factor analysis of variance (ANOVA) to a significance

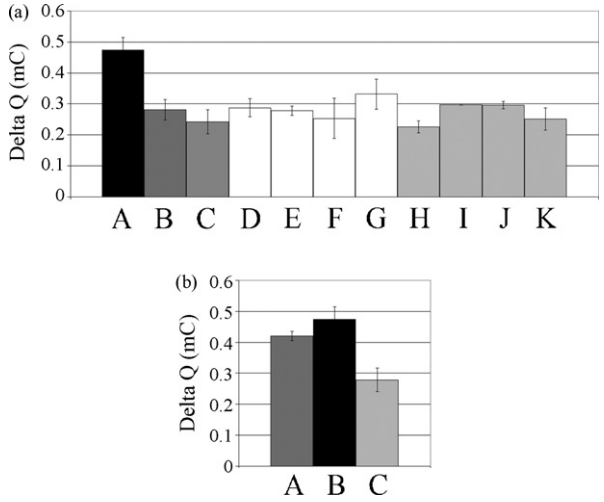

Fig. 2. Cyclic voltammetry results. (a) H5 concentration study as a function of preparation method and comparison to negative controls, as numbered and described in Table 2. Group (A) 2, (B) 3, (C) 4, (D) 7, (E) 6, (F) 5, (G) 8, (H) 9, (I) 10, (J) 11, and (K) 12. (b) Response for H5 1.4 μM using different preparation methods. (A) 1, (B) 2, and (D) 13. For the respective samples, mean $\Delta Q \pm$ SD, $n = 3$ (SD, standard deviation and n, no. of replicates).

Table 2
Average signal of the H5 biosensor for samples tested by preconcentration method.

Group	Reagents	Mean $\Delta Q \pm$ SD ($n = 3$) (mC)
1	[3′SLe^x 100 μM + H5 1.4 μM) + anti-H5–EAM	0.42050 ± 0.0087^a
2	[3′SLe^x 100 μM + (H5 1.4 μM + 10% mouse serum)] + anti-H5–EAM	0.47444 ± 0.0230^b
3	[3′SLe^x 100 μM + (H5 700 nM + 10% mouse serum)] + anti-H5–EAM	0.28153 ± 0.0188^c
4	[3′SLe^x 100 μM + (H5 360 nM + 10% mouse serum)]+ anti-H5–EAM	0.24322 ± 0.0226^c
5	[No glycan + (H5 1.4 μM + 10% mouse serum)] + anti-H5–EAM	0.25331 ± 0.0373^c
6	[3′SLe^x 100 μM + no H5) + anti-H5–EAM	0.27839 ± 0.0089^c
7	[GT3 100 μM + (H5 1.4 μM + 10% mouse serum)] + anti-H5–EAM	0.28812 ± 0.0172^c
8	No glycan + no HA + anti-H5–EAM	0.33222 ± 0.0281^c
9	[3′SLe^x 100 μM + (H1 1.4 μM + 10% mouse serum)] + anti-H5–EAM	0.22594 ± 0.0115^c
10	[3′SLe^x 100 μM + (H1 1.4 μM + 10% mouse serum)] + anti-H1–EAM	0.29739 ± 0.0001^c
11	[No glycan + (H1 1.4 μM + 10% mouse serum)] + anti-H1–EAM	0.29573 ± 0.0068^c
12	No glycan + no HA + anti-H1–EAM	0.25182 ± 0.0207^c
13	[3′SLe^x 100 μM + (H5* 1.4 μM + 10% mouse serum)] + anti-H5–EAM	0.27883 ± 0.0222^d

SD, standard deviation and *n*, no. of replicates.
Mean ΔQ with different superscript letters (a through d) are significantly different at 95% confidence level ($P < 0.05$).

of 95% ($P < 0.05$) (Table A3). The effects of different HAs, glycans, α-HA antibodies, and HA concentration were assessed to calculate the lower detection limit and specificity of the biosensor.

3. Results and discussion

The sensitivity of the biosensor platform was explored with an H5 concentration range (Table 1). The preconcentration preparation method yielded an average ΔQ value of 0.474 mC for the H5 at 1.4 μM binding to 3′SLe^x. H5 at 700 nM and 360 nM displayed significantly decreased ΔQ values which were not statistically different from each other or the negative controls (Fig. 2a(A–C), Tables 2, A3). The same concentrations of glycan and H5 with and without 10% mouse serum yielded similar ΔQ values ($P = 0.0324$) (Fig. 2b(A and B), Tables 2, A3), indicating that magnetic separation was able to fully extract the target HA from serum matrix. In the preconcentration method, Source A H5 was also shown to be a better binder to 3′SLe^x than Source B H5*, though the same strain (Fig. 2b(B and C)). This may be due to the predicted aggregated nature of Source A H5.

Negative controls yielded ΔQ values that were statistically lower than the reading from the H5-specific glycan/H5 interaction, with H5 at 1.4 μM and glycans 3′SLN or 3′SLe^x. Negative controls both with and without H5 were repeatable and statistically similar (Fig. 2a(D–K), Tables 2, A3). The negative controls, including the GT3/H5 interaction, were also statistically lower than the 3′SLe^x/H5 interaction.

The preconcentration method does not lend itself to blocking with avidin and biotin, since all of the interaction partners, including glycan, HA, and anti-HA–EAM are applied to the SPCE

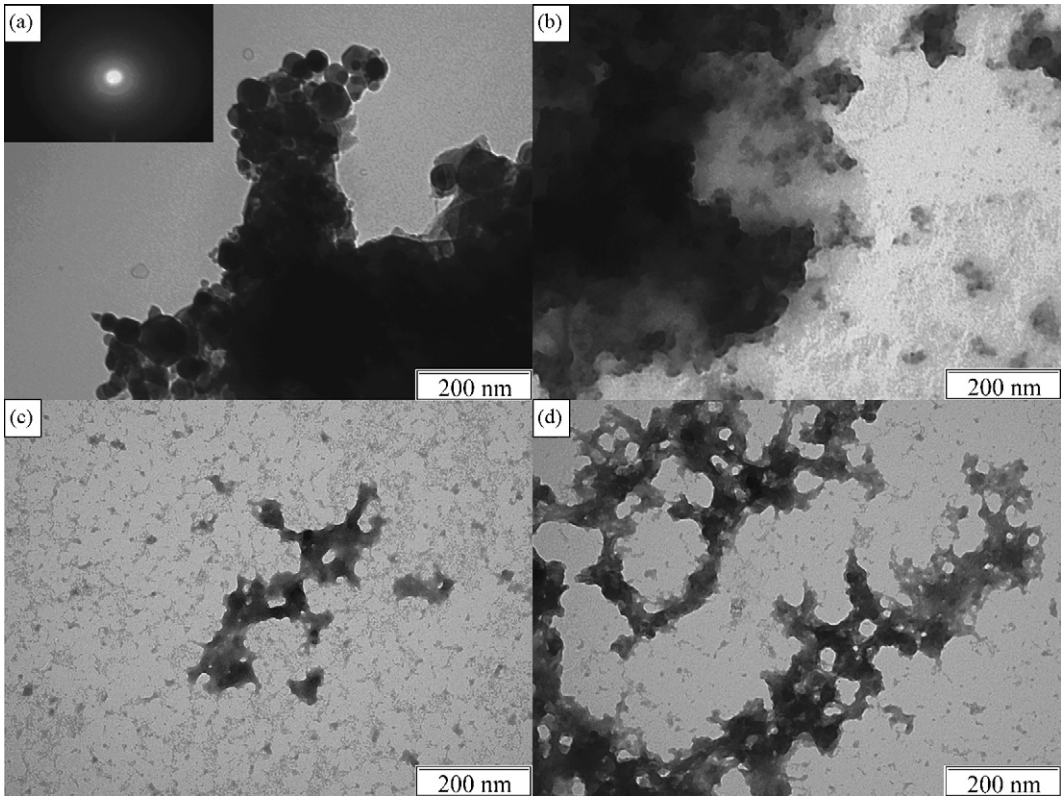

Fig. 3. TEM imaging. (a) TEM and electron diffraction micrograph (inset) of EAM polyaniline nanoparticles with gamma iron(III) oxide cores, (b) TEM of EAMs immunofunctionalized with α-H5 antibody, (c) 3′SLe^x/H5/α-H5–EAM complex, magnetically separated and washed, with H5 prepared with 10% mouse serum, and (d) 3′SLe^x/H5/α-H5–EAM complex with H5 prepared without serum.

as a preformed complex. The magnetic separation step is sufficient to eliminate irrelevant material which could interfere with target binding.

The specificity of the system was investigated with H1. H1 at 1.4 μM in 10% mouse serum was preincubated with the H5-specific glycan 3′SLe^x and subsequently incubated with EAMs conjugated with either α-H5 or α-H1 antibodies. The samples containing both H1 and α-H1–EAM complexes showed higher ΔQ as compared to samples without H1 or with α-H5–EAM complexes (Fig. 2a(H–K)). This may indicate that the H1 and α-H1 antibodies interact and cause slightly higher levels of nonspecific binding. However, all H1-based negative controls remain within the statistical range of the H5-based negative controls (Table 2, Table A3). This indicates that despite the polyclonal nature of the α-H1 antibodies, there is little cross-reactivity with the H5-targeted biosensor. The ΔQ values for H5 binding to the H5-nonspecific glycans, GT3 or 6′SLN, were distinguishably lower than their corresponding positive binder, 3′SLe^x or 3′SLN. We conclude that the biosensor is highly specific for H5.

The structural morphologies of the EAM polyaniline nanoparticles, EAMs immunofunctionalized with α-H5 antibody, and glycan/HA/anti-HA–EAM complexes, stained with 1% uranyl acetate, were analyzed by a JEOL (Peabody, MA) 100CX II Transmission Electron Microscope (TEM). The crystalline nature of the EAM nanoparticles was also studied by selected area electron diffraction using the JEOL 2200FS field emission TEM. EAM polyaniline nanoparticle sizes were revealed in the 25–100 nm range (Fig. 3a). The darkest circular areas correspond to the γ-Fe_2O_3 cores surrounded by the lighter colored polyaniline polymerized around the cores. Immunofunctionalization of the EAM nanoparticles yields a cloudier border, indicating that immunofunctionalization was effective (Fig. 3b). TEM imaging of the 3′SLe^x/H5/α-H5–EAM complex after two magnetic separations and washes resulted in a web-like boundary which could be attributed to the binding of the H5 and glycan, forming a more branched complex. When comparing the 3′SLe^x/H5/α-H5–EAM antibody complex prepared with H5 with and without 10% mouse serum, the TEM images reveal similarly shaped aggregates, indicating no nonspecific serum binding (Fig. 3c and d). Sample prepared with mouse serum has a cloudier supernatant, suggesting the benefit of a more thorough washing, although the ΔQ values are not affected.

Further work is required to optimize biosensor sensitivity for HA detection at concentrations reflecting the viral load in an influenza infected patient. Preconcentration of target analyte is a viable option. Nonspecific binding can be further reduced by improving blocking techniques or wash steps. The specificity, affordability, portability, and repeatability of our novel emerging technology are promising. The biosensor design is easily adaptable to detection of other FLUAV strains, including the current swine-origin H1N1.

4. Conclusion

This study describes a novel design which utilizes electrically active magnetic nanoparticles both as magnetic separator and biosensor transducer. The biosensor system is rapid to results, with 10 min signal detection time and 75 min sample preparation time. SPCEs may be prepared 3 months in advance. The sensitivity of the biosensor in the detection of recombinant H5 (H5N1 A/Vietnam/1203/04) was found to be 1.4 μM in 10% mouse serum. The biosensor demonstrates high avidity of binding between H5 and α2,3-linked glycans 3′SLe^x and 3′SLN with statistically lower binding between H5 and α2,6-linked 6′SLN and α2,8-linked GT3, which is confirmatory to expected results and demonstrates that the biosensor can characterize HA by sialic acid receptor preference. The biosensor showed high specificity for H5 as compared to H1 (H1N1 A/South Carolina/1/18). Our results indicate that the biosensor technology is valuable as a rapid, specific, and sensitive detection method with point-of-care applicability for identifying pandemic avian influenza viruses with α2,3 specificity. We expect that the biosensor system can be easily modified to similarly detect α2,6-specific HAs, an indicator of human pandemic potential. We have demonstrated the ability of the EAMs to immunomagnetically separate target HA from serum matrix, which will be useful for testing serum or respiratory secretions. The development of such a biosensor technology which identifies FLUAV HA based on specificity to host sialic acids is significant to disease monitoring and homeland security.

Acknowledgements

This work was supported by Critical Path Funding from the U.S. Food and Drug Administration, Center for Biologics Evaluation and Research (FDA CBER). "The findings and conclusions in this publication have not been formally disseminated by the Food and Drug Administration and should not be construed to represent any Agency determination or policy."

The authors thank E.B. Setterington for cyclic voltammetry reagents and E. Torres-Chavolla, A. Pastor-Lecha, and the Center for Advanced Microscopy, Michigan State University, for providing TEM expertise. We also thank Dr. N. Razi and A. Tran-Crie of the Carbohydrate Synthesis/Protein Expression Core and Dr. D. Smith of the Protein-Carbohydrate Interaction Core of The Consortium for Functional Glycomics for assistance with synthetic biotinylated carbohydrates.

Appendix A. Supplementary data

Supplementary data associated with this article can be found, in the online version, at doi:10.1016/j.bios.2010.07.047.

References

Ahuja, T., Mir, I.A., Kumar, D., Rajesh, 2007. Biomaterials 28 (5), 791–805.
Amano, Y., Cheng, Q., 2005. Anal. Bioanal. Chem. 381, 156–164.
Baker, C., Shah, S.I., Hasanain, S.K., 2004. J. Magn. Magn. Mater. 280, 412–418.
Blixt, O., Head, S., Mondala, T., Scanlan, C., Huflejt, M.E., Alvarez, R., Bryan, M.C., Fazio, F., Calarese, D., Stevens, J., Razi, N., Stevens, D.J., Skehel, J.J., van Die, I., Burton, D.R., Wilson, I.A., Cummings, R., Bovin, N., Wong, C.-H., Paulson, J.C., 2004. Proc. Natl. Acad. Sci. U.S.A. 101 (49), 17033–17038.
Catolla, J., Atillo, A., Smyth, M.R., 2006. Talanta 68, 1591–1600.
Dallas, P., Moutis, N., Devlin, E., Niarchos, D., Petridis, D., 2006. Nanotechnology 17, 5019–5026.
Daniel, M.-C., Astruc, D., 2004. Chem. Rev. 104, 293–346.
Dominguez Renedo, O., Alonso-Lomillo, M.A., Arcos Martinez, M.J., 2007. Talanta 73, 202–219.
D'Souza, S.F., 2001. Biosens. Bioelectron. 16, 337–353.
Faix, D.J., Sherman, S.S., Waterman, S.H., 2009. N. Engl. J. Med. 361 (7), 728–729.
Gurtler, L., 2006. In: Kamps, B.S., Hoffmann, C., Preiser, W. (Eds.), Influenza Report 2006. Flying Publisher, Paris, pp. 48–86.
Hill, H.D., Mirkin, C.A., 2006. Nat. Protoc. 1, 324–336.
Homeland Security Council (HSC), 2005. National strategy for pandemic Influenza. Available at: http://www.whitehouse.gov/homeland/nspi.pdf (accessed 5.04.09).
Kuwabata, S., Nakano, H., Tachibana, Y., 2005. Proc. 207th Meeting Electrochem. Soc., p. 1728.
Kuznetsov, A.M., 1995. Charge Transfer in Physics, Chemistry, and Biology: Physical Mechanisms of Elementary Processes and an Introduction to the Theory. Overseas Publishers Association, Amsterdam.
Lin, Y.-H., Chen, S.-H., Chuang, Y.-C., Lu, Y.-C., Shen, T.Y., Chang, C.A., Lin, C.-S., 2008. Biosens. Bioelectron. 23, 1832–1837.
Magalhaes, R.J.S., Ortiz-Pelaez, A., Thi, K.L.L., Dinh, Q.H., Otte, J., Pfeiffer, D.U., 2010. BMC Vet. Res. 6 (10), 1–10.
Michaelis, M., Doerr, H.W., Cinatl Jr., J., 2009. Med. Microbiol. Immunol. 198 (3), 175–183.
Muhammad-Tahir, Z., Alocilja, E.C., Grooms, D.L., 2007. Sensors J. 7, 1123–1140.
Neumann, G., Chen, H., Gao, G.F., Kawaoka, Y., 2010. Cell Res. 20 (1), 51–61.
Pal, S., Alocilja, E.C., 2009. Biosens. Bioelectron. 24, 1437–1444.
Pal, S., Alocilja, E.C., Downes, F.P., 2007. Biosens. Bioelectron. 22, 2329–2336.
Pal, S., Setterington, E., Alocilja, E.C., 2008a. IEEE Sensors J. 8 (6), 647–654.
Pal, S., Ying, W., Alocilja, E.C., Downes, F.P., 2008b. Biosyst. Eng. J. 99 (4), 461–468.

Poddar, P., Wilson, J.L., Srikanth, H., Morrison, S.A., Carpenter, E.E., 2004. Nanotechnology 15, S570–S574.
Reid, A.H., Taubenberger, J.K., Fanning, T.G., 2001. Microbes Infect. 3, 81–87.
Sarno, D.M., Manohar, S.K., Macdiarmid, A.G., 2005. Synth. Met. 148, 237–243.
Scott, M.T., Spinks, G.M., Wallace, G., 2005. Sens. Actuators B: Chem. 107, 657–665.
Sharma, R., Lamba, S., Annapoorni, S., Sharma, P., Inoue, A., 2005. J. Appl. Phys. 97 (1), 14311–14316.
Stevens, J., Blixt, O., Glaser, L., Taubenberger, J.K., Palese, P., Paulson, J.C., Wilson, I.A., 2006. J. Mol. Biol. 355, 1143–1155.
Susmel, S., Guilbault, G.G., O'Sullivan, C.K., 2003. Biosens. Bioelectron. 18, 881–889.
Turner, A.P.F., Karube, I., Wilson, G.S., 1987. Biosensors Fundamentals and Applications. Oxford University Press, Oxford, UK.
Webster, R.G., Bean, W.J., Gorman, O.T., Chambers, T.M., Kawaoka, Y., 1992. Microbiol. Rev. 56, 152–179.
Werner, O., Harder, T.C., 2006. In: Kamps, B.S., Hoffmann, C., Preiser, W. (Eds.), Influenza Report 2006. Flying Publisher, Paris, pp. 48–86.
Wiley, D.C., Skehel, J.J., 1987. Ann. Rev. Biochem. 56, 365–394.
Willner, I., Baron, R., Willner, B., 2007. Biosens. Bioelectron. 22, 1841–1852.
World Health Organization (WHO), 2002. WHO Manual on Animal Influenza Diagnosis and Surveillance. Available at: http://www.who.int/vaccine_research/diseases/influenza/WHO_manual_on_animal-diagnosis_and_surveillance_2002_5.pdf (accessed 2.06.10).
World Health Organization (WHO), 2007a. Collecting, Preserving and Shipping Specimens for the Diagnosis of Avian Influenza A (H5N1) Virus Infection: Guide for Field Operations; 2007. Available at: http://www.who.int/csr/resources/publications/surveillance/whocdscsredc2004.pdf (accessed 20.12.07).
World Health Organization (WHO), 2007b. Recommendations and Laboratory Procedures for Detection of Avian Influenza A (H5N1) Virus in Specimens from Suspected Human Cases 2007. Available at: http://www.who.int/csr/disease/avian_influenza/guide-ines/RecAllabtestsAug07.pdf (accessed 1.05.08).
World Health Organization (WHO), 2009. Continuing Progress Towards a Unified Nomenclature System for the Highly Pathogenic H5N1 Avian Influenza Viruses. Available at: http://www.who.int/csr/disease/avian_influenza/guidelines/nomenclature/en/index.html (accessed 12.03.10).
Wright, P.F., Webster, R.G., 2001. In: Knipe, D.M., Howley, P.M. (Eds.), Fields Virology, 4th ed. Lippincott Williams & Wilkins, Philadephia, pp. 1533–1579.
Xue, W., Fang, K., Qiu, H., Li, J., Mao, W., 2006. Synth. Met. 156, 506–509.
Zhang, D., Carr, D., Alocilja, E.C., 2009. Biosens. Bioelectron. 24, 1377–1381.
Zhang, Z., Wan, M., Wei, Y., 2005. Nanotechnology 16, 2827–2832.